Secretory-granule dynamics visualized *in vivo* with a phogrin–green fluorescent protein chimaera

Aristea E. POULI*, Evaggelia EMMANOUILIDOU*, Chao ZHAO*, Christina WASMEIER†, John C. HUTTON†, and Guy A. RUTTER*[1]

*Department of Biochemistry, School of Medical Sciences, University Walk, University of Bristol, Bristol BS8 1TD, U.K., and †Barbara Davis Center for Childhood Diabetes, University of Colorado Health Services Center, Box B140, 4200 East, 9th Avenue, Denver, CO 80262, U.S.A.

To image the behaviour in real time of single secretory granules in neuroendocrine cells we have expressed cDNA encoding a fusion construct between the dense-core secretory-granule-membrane glycoprotein, phogrin (phosphatase on the granule of insulinoma cells), and enhanced green fluorescent protein (EGFP). Expressed in INS-1 β-cells and pheochromocytoma PC12 cells, the chimaera was localized efficiently (up to 95 %) to dense-core secretory granules (diameter 200–1000 nm), identified by co-immunolocalization with anti-(pro-)insulin antibodies in INS-1 cells and dopamine β-hydroxylase in PC12 cells. Using laser-scanning confocal microscopy and digital image analysis, we have used this chimaera to monitor the effects of secretagogues on the dynamics of secretory granules in single living cells. In unstimulated INS-1 β-cells, granule movement was confined to oscillatory movement (dithering) with period of oscillation 5–10 s and mean displacement $< 1\ \mu$m. Both elevated glucose concentrations (30 mM), and depolarization of the plasma membrane with K^+, provoked large (5–10 μm) saltatory excursions of granules across the cell, which were never observed in cells maintained at low glucose concentration. By contrast, long excursions of granules occurred in PC12 cells without stimulation, and occurred predominantly from the cell body towards the cell periphery and neurite extensions. Purinergic-receptor activation with ATP provoked granule movement towards the membrane of PC12 cells, resulting in the transfer of fluorescence to the plasma membrane consistent with fusion of the granule and diffusion of the chimaera in the plasma membrane. These results illustrate the potential use of phogrin–EGFP chimeras in the study of secretory-granule dynamics, the regulation of granule–cytoskeletal interactions and the trafficking of a granule-specific transmembrane protein during the cycle of exocytosis and endocytosis.

INTRODUCTION

Glucose activates exocytosis of insulin from islet β-cells through an increase in intracellular free [Ca^{2+}], prompting the fusion of granules located close to or docked at the plasma membrane [1]. Glucose may also promote the recruitment to the plasma membrane of granules located deeper within the β-cell interior [2,3]. Similarly, in adrenal chromaffin cells, neurotransmitter-induced [Ca^{2+}] increases provoke the release of stored catecholamines [4]. Whether granules remote from the plasma membrane are recruited in this cell type is unclear.

Investigation of granule dynamics in living cells represents a considerable technical challenge. Techniques used in the past include cinematography and video-imaging of the movement of dense bodies (assumed to be secretory granules) in flattened cells, using a phase-contrast light microscope [2,3,5]. Recent studies [6–8] have employed granule-membrane cargo proteins, fused to green fluorescent protein (GFP) [9], to measure vesicle dynamics and exocytosis. However, these studies are hampered by the fact that only a proportion (40 % [8] to 70 % [6]) of the expressed fluorescent reporters are targeted correctly to mature secretory granules. Instead, there is significant retention of the proteins in the endoplasmic reticulum and trans-Golgi network [8] and direction of the proteins to other vesicles, possibly of the non-regulated secretory pathway [6]. This problem is also compounded by the uncertain stability and fluorescence properties of GFP in the low-pH environment of the granule lumen. Although the exocytotic event can be imaged by this approach, it is not possible to monitor the fate of the granule membrane, or membrane proteins, after fusion with the plasma membrane.

To monitor granule movement and exocytosis in single living cells we have constructed a recombinant cDNA encoding a chimaera between the granule-specific transmembrane glycoprotein phogrin (phosphatase on the granule of insulinoma cells) and an enhanced form of green fluorescent protein (EGFP) [9]. Phogrin was originally identified using antibodies to highly enriched insulinoma dense-core granule membranes to probe a rat insulinoma cDNA-expression library [10]. Phogrin (1004 amino acids) is a type 1 transmembrane glycoprotein of mature M_r 60000–64000, consisting of an N-terminal intralumenal domain, a transmembrane domain and a C-terminal cytosolic protein tyrosine phosphatase domain. When expressed in anterior pituitary AtT-20 cells in native form (J. C. Hutton, unpublished work), or as a fusion with aequorin in insulin-secreting INS-1 cells [11], phogrin is sorted efficiently to dense-core secretory granules, which constitute the major intracellular pool of the protein. Fusion of EGFP at the C-terminus of phogrin therefore is predicted to place EGFP exclusively on the outer surface of the granule, exposed to the cytosolic environment.

Using the phogrin–EGFP chimaera, we have examined the behaviour of dense-core secretory granules in two neuroendocrine cell types; islet INS-1 β-cells are a highly differentiated [12] and glucose-sensitive insulinoma cell line that provides a model of islet β-cells [13,14]. Pheochromocytoma cells are derived from

Abbreviations used: phogrin; phosphatase on the granule of insulinoma cells; GFP, green fluorescent protein; EGFP, enhanced green fluorescent protein; D-βH, dopamine β-hydroxylase.

[1] To whom correspondence should be addressed (e-mail g.a.rutter@bris.ac.uk).

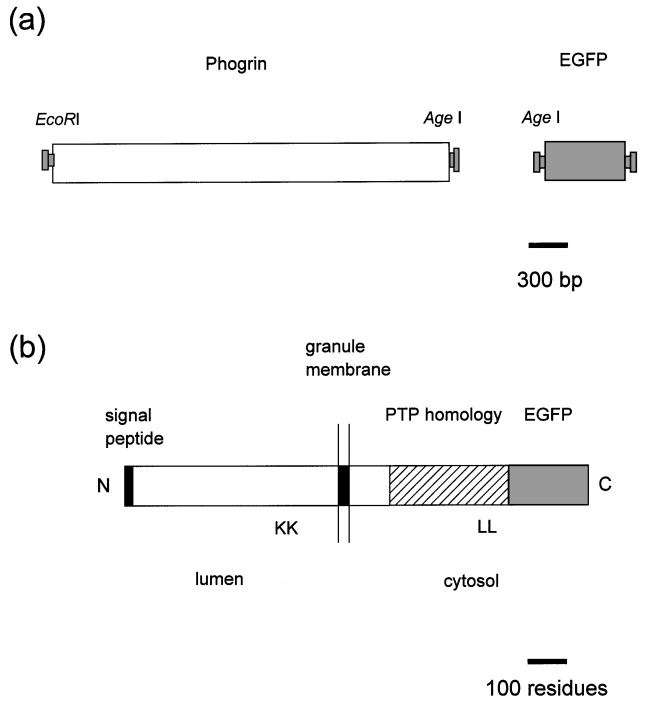

Figure 1 Construction and expression of phogrin–EGFP

(**a**) Strategy for phogrin–EGFP construction. cDNA encoding full-length phogrin, minus TAG stop codon (1003 amino acids), was generated by PCR amplification (see Methods section) with flanking *Eco*R1 and *Age*1 restriction sites. Ligation with *Age*1-digested plasmid pEGFP-N1 produced cDNA encoding the in-frame phogrin–EGFP chimaera. (**b**) Predicted type I membrane topology of the expressed chimaera, with EGFP lying on the cytosolic surface of the granule. The protein tyrosine phosphatase (PTP) domain, likely di-lysine (KK) cleavage site and di-leucine (LL) localization domain are shown.

an adrenal chromaffin cell tumour [15], secrete catecholamines, and are a widely used model of sympathetic neurones. We demonstrate that the phogrin–EGFP chimaera is targeted efficiently to dense-core secretory granules in each of these cell types. This allows the monitoring of granule movement before exocytosis, and the fate of this granule membrane protein after vesicle fusion.

Time-lapse movies accompany this paper, and are presented on the World Wide Web at the URLs given in the Figure legends.

MATERIALS AND METHODS

Materials

Tissue-culture reagents were obtained from Gibco-BRL Ltd. Guinea-pig anti porcine (pro-)insulin antiserum was obtained from Dako Ltd., Bucks, U.K, and rabbit anti-dopamine β-hydroxylase (D-βH) antibodies from Biogenesis (Poole, Dorset, U.K.). Other reagents were from Boehringer Mannheim (Mannheim, Germany) or Sigma (Poole, Dorset, U.K.).

Methods

Plasmid construction

cDNA encoding the entire coding region of phogrin was amplified by PCR using ExpandTaq™ (Boehringer Mannheim) with forward primer 5′-T.TTT.GAA.TTC.GAC.GAG.ATG.GGG.-CTA.CCG.CTC.CG-3′, including an *Eco*R1 restriction site (underlined), and a Kozak sequence, and reverse primer 5′-TTT.TAC.CGG.TCC.CTG.GGG.AAG.GGC.CTT.CAG-3′ (with *Age*1 site underlined). The 3.01 kb PCR product was digested and subcloned into plasmid pN1-EGFP (Clontech) encoding EGFP ($S^{65}T$, $F^{64}L$, and codon-usage mutations) under cytomegalovirus immediate-early gene promoter control.

Cell culture and microinjection

INS-1 [12,14] and PC12 [11] cells were cultured as described previously, on poly-L-lysine (Sigma) or collagen (murine type IV; Becton-Dickinson Labware, MA, U.S.A.)-coated coverslips, respectively. cDNA was introduced by microinjection at 0.35 mg·ml^{-1} in 2 mM Tris/HCl/0.2 mM EDTA (pH 8.0) as described [16]. Following microinjection, cells were incubated for 16–24 h in an atmosphere of 5% CO_2.

Immunocytochemistry

Cells were fixed and permeabilized 24 h after microinjection with 4% (v/v) paraformaldehyde/0.2% Triton X-100. Intrinsic EGFP fluorescence was maintained under these conditions. Primary polyclonal antibodies to (pro-)insulin (1:100 dilution) and to D-βH (1:100 dilution) were revealed with tetramethylrhodamine-conjugated secondary antibodies, in 0.1% (v/v) BSA. Cells were washed with PBS between incubations and mounted on coverslips with Mowiol before analysis. Confocal images were captured using a laser-scanning confocal microscope (Leica TCS 4D/DM IRBE; 63×/1.32 NA PL-Apo oil-immersion lens) equipped with a krypton/argon laser (488 and 568 nm excitation lines), and analysed off-line using Adobe Photoshop 3.0™.

In vivo confocal imaging

Prior to imaging, cells were incubated for 30 min in Krebs-Ringer medium comprising 125 mM NaCl, 3.5 mM KCl, 1.5 mM $CaCl_2$, 0.5 mM $MgSO_4$, 0.5 mM KH_2PO_4, 2.5 mM $NaHCO_3$, 3 mM glucose, and 10 mM $HepesNa^+$ (pH 7.4), equilibrated with a 95:5 O_2:CO_2 mixture. Cells were then transferred to the thermostat-controlled (37 °C) stage of a Leica TCS 4D/DM IRBE inverted-optics confocal microscope, fitted with a 40×/1.0 NA PL Fluotar oil-immersion objective, and controlled by TCS-NT4 software (Leica). Cells were maintained in Krebs-Ringer medium (0.5 ml), which was replaced with the same medium but containing additions (pre-warmed to 37 °C) when required (exchange time < 15 s). Two scans were performed for each image; this allowed capture of images of sufficient quality for image analysis every 5 s, and ensured minimum bleaching of EGFP fluorescence. Laser power did not exceed 50% and typical pinhole sizes and photomultiplier gains were 0.4 μm and 500–580/1000, respectively.

Image analysis

Images were exported as TIFF files and processed using Adobe Photoshop 3.0™. After conversion of files to GIF format (PaintShop Pro), time-lapse image sequences were prepared using a GIF construction set (Shareware, URL http://www.mindshop.com). Scale bars were calculated using the Leica software; in a typical experiment (40× objective magnification, 4× zoom) the 512×512-pixel image corresponded to a 60×60 μm box (i.e. 0.117 μm pixel width).

Granule movement was analysed using NIH Image (freeware from ftp://zippy.nimh.nih.gov/pub/image/) and GIF construction sets. The velocity of individual granules was calculated from the movement between successive images.

Insulin radio-immunoassay

INS-1 cells were cultured, for 48 h in 96-well microtitre plates, before the assay of insulin release in Krebs-Ringer medium (for details see above) [13] by competitive radio-immunoassay (Linco Res. Inc., MO, U.S.A.).

Statistical analysis

Data are given as the mean ± S.E.M. for the number of observations shown. Statistical significance was calculated with paired Student's *t*-tests, assuming equal variances.

RESULTS

Imaging granule movement in INS-1 β-cells with expressed phogrin–EGFP

The structure of the chimaeric phogrin–EGFP cDNA construct, and the domain structure and predicted topology of the expressed recombinant protein, are shown in Figure 1.

Using immuno-electron microscopy and an incorporated epitope tag, we have demonstrated previously that a chimaera similar to phogrin–EGFP, phogrin aequorin [11], is targeted efficiently at (pro-)insulin-containing granules in INS-1 cells. In the present study, we used confocal microscopy to determine the subcellular distribution of the intrinsic fluorescence of the phogrin–EGFP chimaera, compared with that of immunostained insulin. This approach was complicated by the fact that permeabilization adequate to allow labelling of secretory granules with anti-insulin antibodies caused a loss of EGFP-derived fluorescence. Thus, strong EGFP-derived fluorescence was usually observed in cells that were not labelled with anti-insulin antibodies. Nevertheless, under optimal permeabilization conditions, expressed phogrin–EGFP was localized in INS-1 cells to > 95 % of insulin-containing vesicles (Figures 2a–c). However, approx. 60 % co-localization to (pro-)insulin-containing structures (Figures 2d–f) was observed more usually, as a result of the above limitation. In cells where close co-localization between the chimaera and insulin was revealed, we could not detect phogrin–EGFP-positive, insulin-negative, nor phogrin–EGFP-negative, insulin-positive structures (data taken from > 50 individual INS-1 cells from 4 separate cultures). However, there were significant differences in the ratio of phogrin : insulin-derived

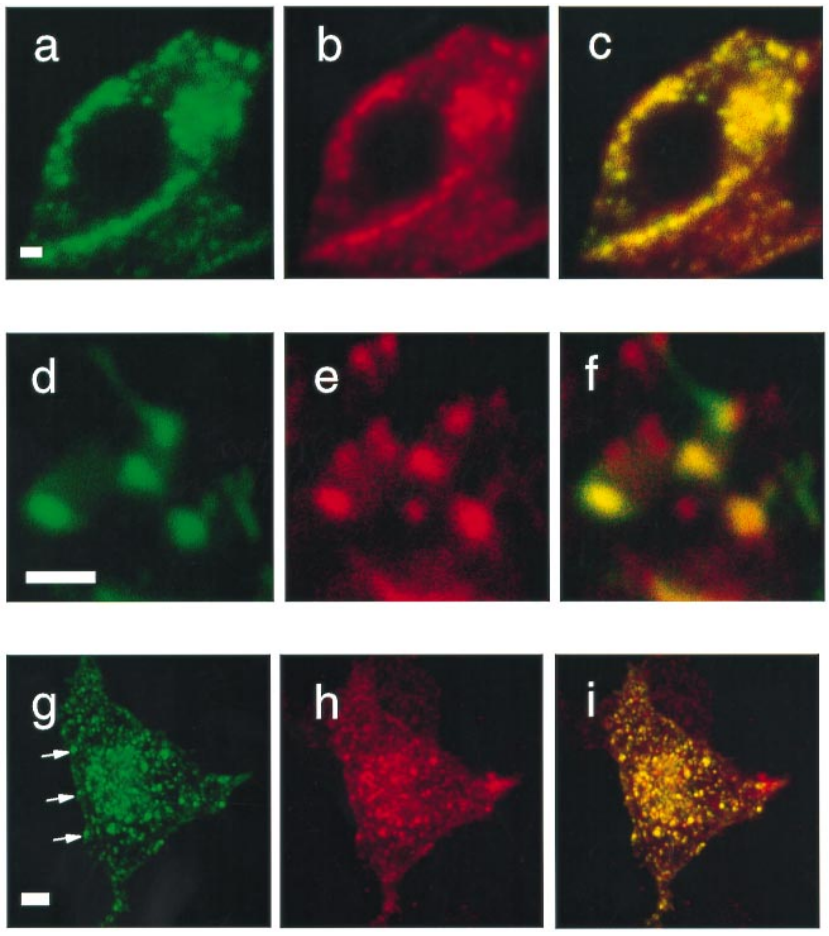

Figure 2 Localization of phogrin–EGFP to dense-core secretory vesicles in INS-1 and PC12 cells

(**a**–**c**) Co-localization with (pro-)insulin in INS-1 β-cells. Cells expressing phogrin–EGFP were fixed and probed with polyclonal anti-(pro-)insulin antiserum, followed by tetramethyl-rhodamine (TRITC)-conjugated rabbit anti-guinea-pig IgG as secondary antibody. (**a**) Intrinsic EGFP fluorescence (488 nm excitation); (**b**) TRITC-fluorescence (568 nm excitation); (**c**) overlay of (**a**) and (**b**). (**d**, **e**) As (**a**–**c**) but with a different individual cell, examined at higher magnification (scale bar = 1 μm). (**f**) Overlay of (**d**) and (**e**). (**g**–**i**) Co-localization of phogrin–EGFP with D-βH in fixed PC12 cells probed with polyclonal rabbit anti-D-βH primary antibody, and TRITC-conjugated anti-rabbit IgG as secondary antibody. Note the close colocalization observed in the arrowed granules. Scale bars = 2 μm.

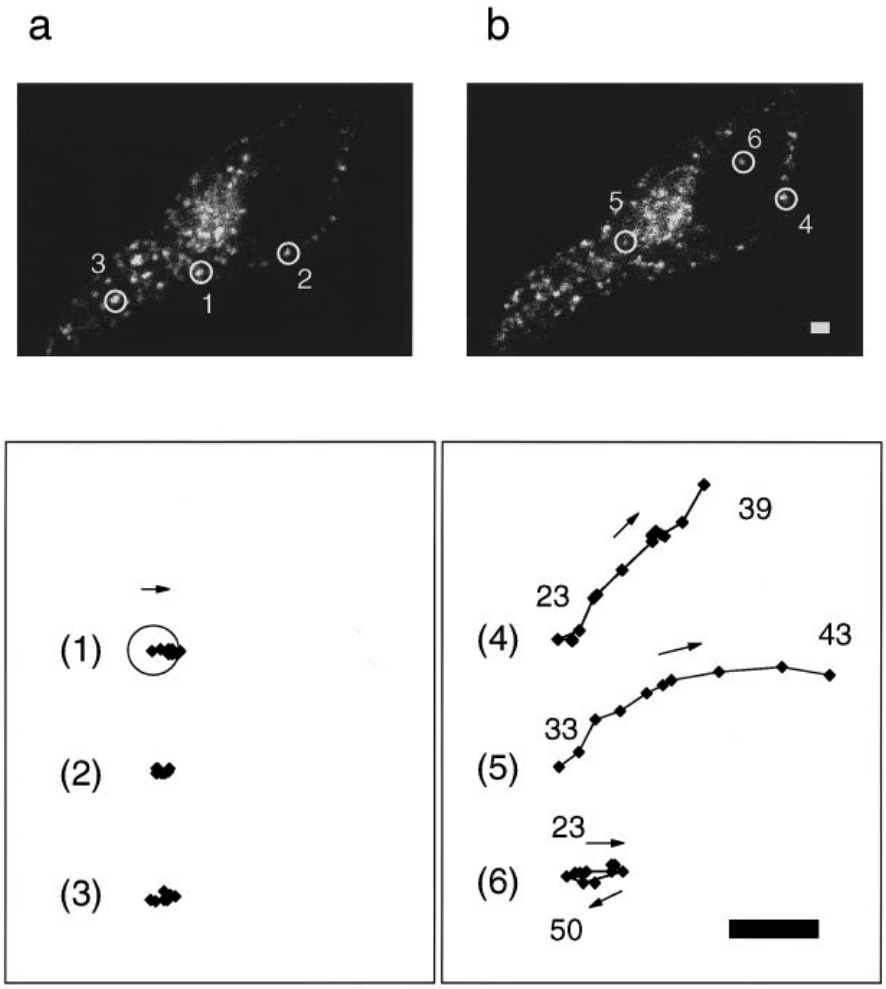

Figure 3 Effect of glucose on dense-core secretory-vesicle dynamics in living INS-1 cells

Fluorescence was monitored in a single INS-1 cell expressing phogrin–EGFP, by scanning confocal microscopy. Images were the mean of two scans obtained within a 5 s interval, as described in the Methods section. (**a**) One image of 15 obtained in the presence of 3 mM glucose; (**b**) Image 16 of 35 obtained after addition of 30 mM glucose. Images were corrected off-line for progressive fluorescence loss by photobleaching (approx. 20% during the course of the experiment). These images are presented as time-lapse movies that can be accessed through the World Wide Web by connecting to URL: http://www.BiochemJ.org/bj/333/bj3330193add.htm. The presence of glucose at 30 mM is indicated in the time-lapse movie. The movement of the individual granules shown (lower panels) was plotted from the obtained confocal images using NIH Image. The initial position of the centre of each granule (approx. size indicated by the circle) was that in image 1 (left panel, 3 mM glucose). In the right panel (30 mM glucose), numbers indicate the frame number in which the granule occupied the position shown. Scale bars = 2 μm.

fluorescence between individual granules (Figure 2, a versus b). The dimensions of the doubly labelled structures (200–500 nm) corresponded closely with those of dense-core secretory vesicles [17].

The majority of granules that could be observed in the focal plane (approx. 500 nm deep) of an individual living INS-1 cell displayed linear, back-and-forth movements, with a period (5–7 s) close to that of the rate of data acquisition (Figure 3). The amplitude of these movements was within 2–3 times the diameter of the granule. Analysis of the movement of granules in a further single cell is presented in Table 1. Maintained in low glucose concentration (3 mM), no granule was observed to move more than 1 μm (approx. 5 granule diameters) from its point of origin during a typical 2.5 min observation (data taken from 18 individual cells from separate cultures). Elevation of the glucose concentration to 30 mM, sufficient to provoke a 2.2-fold increase in insulin release from cell populations (Table 1), increased markedly the movement of the granules (Figure 3; Table 1). Under these conditions, it was possible to detect the movement of individual granules over much longer distances (up to 5 μm). For example, elevation of glucose concentration provoked the excursion of two granules in the cell shown in Figure 3(b) (granules #4 and #5). In this experiment, granules can also be seen to be moving in and out of the focal plane (i.e. along the z axis) after the addition of 30 mM glucose. In seven out of eight separately cultured cells examined in the presence of 30 mM glucose, the movement of two or more granules in this manner was detectable in a 2.5 min data-acquisition period.

This effect of glucose was also mimicked by cell depolarization provoked with 70 mM KCl. Measured in cell populations, stimulation with high K^+ concentration (56 mM), led to a 2.7-fold stimulation of insulin release (Table 1). In Figure 4, a single INS-1 cell was maintained initially in the presence of 3 mM glucose before the addition of 70 mM K^+ (indicated in the time-lapse movie). The granule in the centre of the cell (over the nuclear region, granule #5) remains fixed during three acquisition

Table 1 Effect of glucose and KCl on granule movement and insulin secretion in INS-1 cells

Granule movement was determined for a single INS-1 cell. Individual granules were identified and the maximum distance moved (in granule diameters) by each granule from its starting position was calculated during 15 data acquisitions (75 s). The number of individual granules examined is given in parentheses. High [KCl] = 70 mM (granule movement) or 56 mM (insulin release). Insulin release (ng of insulin · 100 000 cells^{-1} · 30 min^{-1}) was measured in four separate cultures. $^{*}p < 0.05$, $^{***}p < 0.001$ for the effect of 30 mM glucose.

Concentration (glucose or K^+)	Granule movement (diameters)	Insulin secretion
3 mM glucose	0.7 ± 0.17 (26)	9.1 ± 2.1
30 mM glucose	3.2 ± 0.58*** (20)	17.1 ± 2.3*
3 mM glucose	1.08 ± 0.26 (15)	9.1 ± 2.1
3 mM glucose + high KCl	4.42 ± 2.03* (13)	24.5 ± 2.4*

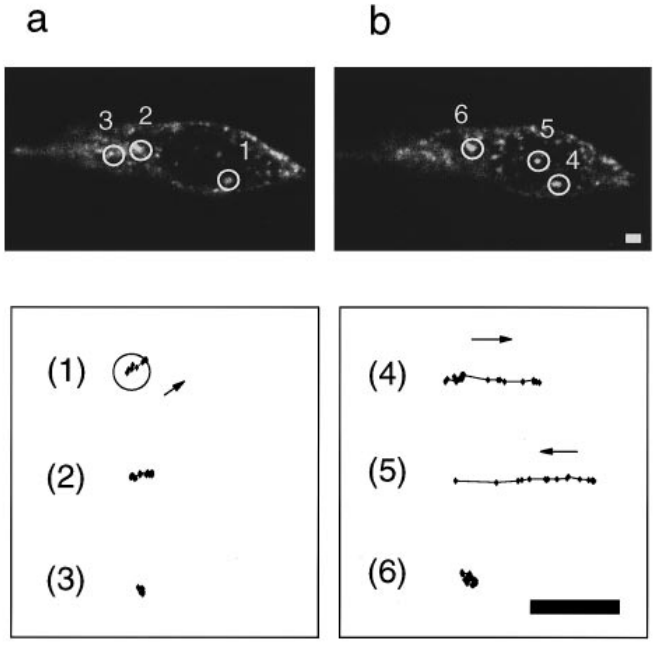

Figure 4 Effect of K^+ on secretory-vesicle dynamics in living INS-1 cells

Fluorescence was monitored as described in the Figure 3 legend. (**a**) Image 1 of 15 acquired in the presence of 3 mM glucose alone. (**b**) Image 1 of 24, obtained in the presence of 70 mM KCl. Note the movement of the indicated granules (see the Results section for further details). Bleaching of fluorescence was minimal in this experiment, and the images are shown as raw data. These images are presented as time-lapse movies that can be accessed through the World Wide Web by connecting to URL: http://www.BiochemJ.org/bj/333/bj3330193add.htm. Movement of the indicated granules is shown in the corresponding panels. Scale bars = 2 μm.

periods after K^+ addition, before moving approx. 2 μm in the next three frames, pausing and then moving approx. 4 μm in the next three frames. This represents a maximum velocity of approx. 0.2 μm · s^{-1}. Similar behaviour was noted in a further granule (#4), whereas a third (#6) barely moved from its point of origin.

No clear evidence of fusion of phogrin–EGFP-containing granules with the plasma membrane was apparent in INS-1 cells. This may reflect either (i) the relatively low exocytotic activity of this cell type, or (ii) a transient interaction between phogrin–EGFP and the plasma membrane, which does not lead to net accumulation of fluorescence. We therefore sought evidence for membrane fusion in an alternative neuroendocrine cell type, PC12 cells, which exhibit a substantially higher secretion rate in terms of percentage loss of cellular hormone content over time.

Granule movement and exocytosis in PC12 cells

We have reported previously [11] that PC12 cells respond dramatically to stimulation with the purinergic receptor agonist, providing robust exocytosis, monitored by the recruitment to the plasma membrane of the lipophilic dye, FM1-43 [18]. Phogrin–EGFP was targeted efficiently to dense-core granules in PC12 cells, again co-localizing closely with the dense-core granule marker, D-βH (Figures 2d–f). In these cells, which had evident neurite extensions, movement of vesicles from the centre of the cells and into the neurites was clearly apparent, even in this absence of a stimulus (Figure 5a). The maximum velocity achieved in these long excursions was similar to that of INS-1 granules, i.e. approx. 0.2–0.5 μm · s^{-1}. Stimulation of PC12 cells with ATP activates P_{2U} purinergic receptors and produces sustained increases in intracellular [Ca^{2+}] [11]. ATP challenge caused apparently directed movement of granules towards the plasma membrane (Figure 5b). This led to a clear increase in plasma-membrane luminescence (Figure 5, c versus b), presumably the result of the arrival and diffusion of the labelled phogrin during exocytosis, followed by diffusion into the plasma membrane.

DISCUSSION

We have compared the dynamics of vesicle movements in INS-1 β-cells and PC12 neurones, using a phogrin–EGFP chimaera. This chimaera was targeted to secretory vesicles in both cell types, causing the intense fluorescence of individual granules. This allows granule movement to be monitored readily by laser-scanning confocal microscopy. As such, the technique offers a number of advantages over those used previously to monitor granule movement and exocytosis in living β-cells. The complete co-localization of the chimaera with insulin or D-βH eliminates concerns about the identity of the observed granule, a problem which hampers the use of cargo proteins to target GFP to granules [6–8]. Compared with phase-contrast video-microscopy, the use of phogrin–EGFP only detects the movement of granules, with other dense-core bodies (lysosomes, for example) being unlabelled. Furthermore, the use of digital confocal imaging allows analysis of cells with unflattened morphology, which is difficult or impossible with phase-contrast microscopy [2]. Finally, this technique allows conventional confocal microscopy to be employed to monitor the recruitment of a vesicle-membrane protein to the plasma membrane during exocytosis. This eliminates the need for specialized evanescence-wave approaches [6].

In the two cell types examined, the behaviour of secretory granules was quite distinct, both in unstimulated cells and after stimulation with [Ca^{2+}]-raising secretagogues. In unstimulated INS-1 β-cells, granule movement was confined to small oscillatory movements, typically of less than 2–3 granule diameters from the starting location during a 2.5 min observation period. High glucose or K^+ concentrations increased the likelihood of these movements (Table 1), and also provoked longer, saltatory excursions of the granules (Figures 3 and 4). These appeared linear, undirected, and occurred with equal probability towards or away from the plasma membrane. Since these movements can only be detected if they occur in the focal plane, our observation of up to three granules making this movement per cell is a

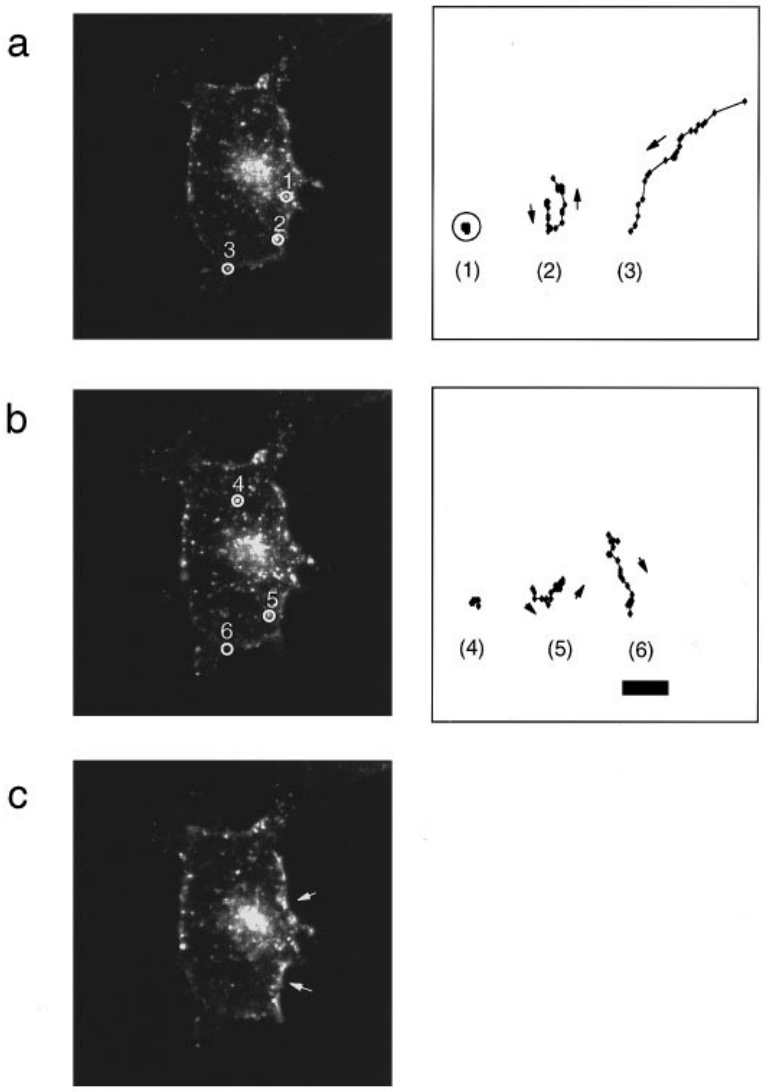

Figure 5 Effect of ATP on secretory-granule dynamics in living PC12 cells

Vesicle dynamics were measured by image acquisition at 5 s intervals in a cell incubated (**a**) in unmodified Krebs-bicarbonate medium containing 3 mM glucose (image 1 of 30; note the movement of vesicles towards neurite extensions; granule #3); (**b**) after the addition of 50 μM ATP (image 1 of 30); or (**c**) 175 s after the addition of ATP (image 30 of 30). Note the accumulation of membrane fluorescence after stimulation with ATP (29 and 62.5% increases in a 30 $\times$ 50-pixel box corresponding to the regions marked by the upper and lower arrows, respectively). A smaller (19%) increase in fluorescence was also apparent in the perinuclear region, whereas a decrease (21%) was observed in a region of the cell distant from the nucleus (in the bottom left of the image). Scale bar = 2 μm. These images are presented as time-lapse movies that can be accessed through the World Wide Web by connecting to URL: http://www.BiochemJ.org/bj/333/bj3330193add.htm.

considerable underestimate of the total number occurring throughout the whole cell. These movements are likely to represent the previously described motion of secretory vesicles in islet β-cells [2,3], most probably along microtubular tracks [19]. An intriguing possibility is that the pauses during movements might correspond to the transfer of a granule between successive microtubular tracks.

The rate of movement of the granules measured in these studies with phogrin–EGFP were comparable with those measured by video microscopy in long-term cultures of islet β-cells [2,3] and in the HIT-T15 β-cell line [5]. Although it is impossible to be certain that the measurements made in the earlier studies described only the movement of secretory granules (and not other dense bodies such as lysosomes), the fact that similar behaviour could be detected in granules bearing phogrin–EGFP suggests that the expressed chimaera did not interfere with the machinery responsible for granule movement. Furthermore, in the current studies with INS-1 β-cells, the effect of increasing glucose from 3 to 30 mM (Figure 3; Table 1) was more dramatic than observed in earlier work [2,3] and exceeded the stimulation of exocytosis measured in cell populations. In particular, we failed to observe any long saltatory granule movements in unstimulated INS-1 cells. This suggests that these may play an important role in the activation of exocytosis by nutrient secretagogues, including glucose. Consistent with an important role for glucose-induced increases in intracellular [Ca^{2+}], the effects of glucose could be mimicked by the activation of Ca^{2+} influx by cell depolarization with KCl.

By contrast, long saltatory granule movements were apparent in PC12 cells even in the absence of intracellular [Ca^{2+}]-raising

agents (Figure 5). These appeared to be directed from the cell interior outwards, i.e. towards the plasma membrane and into neurite extensions. This apparent, predominantly anterograde, movement is therefore compatible with previous observations in which the movement of acidic granules was monitored by enhanced video microscopy after loading AtT-20 cells with acridine orange [20]. This technique, which involved fixation *post-facto* and immunocytochemistry to reveal adrenocorticotrophin-containing granules, indicated that the majority of these secretory granules moved in the anterograde direction. In further agreement with the results of Kreis et al. [20], we also observed that phogrin–EGFP-labelled vesicles undergoing long saltatory jumps did not usually change direction (Figures 5a and 5b, granules #3 and #6). Such behaviour is suggestive of movement along linear microtubules, driven by anterograde motors. Nevertheless, shorter excursions were associated with reversal of direction (Figures 5a and 5b, granules #2 and #5), indicating that 'hopping' between microtubules could occur under these circumstances.

In our studies, increases in intracellular [Ca^{2+}] provoked with ATP apparently increased the number of directed movements of vesicles in PC12 cells. This resulted in clear increases in fluorescence associated with the plasma membrane (Figures 5b and 5c). Thus, secretion in PC12 cells appeared to be associated with the recruitment of the secretory-vesicle granule protein phogrin into the membrane. In this respect, the behaviour of phogrin–EGFP may be similar to that of the granule membrane protein D-βH, examined in intact chromaffin cells [21].

In summary, we describe a new method of selectively monitoring dense-core secretory-granule movement in single living neuroendocrine cells. This involves the use of a granule-membrane-located EGFP fusion protein, and laser-scanning confocal microscopy. This approach reveals important differences in the behaviour of secretory granules in islet INS-1 β-cells and in a model of sympathetic neurones, the PC12 cell. These differences may be related to the regulation of secretion from these cell types by distinct secretagogues *in vivo*, i.e. responsiveness of β-cells to nutrient secretagogues plus modulatory neurotransmitters [22], and of chromaffin cells to neurotransmitters alone. The molecular basis of these differences remains unknown, and will require analysis of the motor and other proteins involved in the transport of secretory granules in these cell types [19].

Received 13 March 1998/14 April 1998; accepted 24 April 1998

We thank the Wellcome Trust, the Medical Research Council (U.K.), the Royal Society, the British Diabetic Association, the Juvenile Diabetes Foundation and the Christine Wheeler Bequest for financial support. We also thank the Medical Research Council for providing an Infrastructure Award to establish the Bristol School of Medical Sciences Cell Imaging Facility, and Dr M. Jepson, A. Leard and E. Basham for technical assistance. A. E. P. is a Bristol University Research Scholar.

REFERENCES

1 Ashcroft, F. M. and Kakei, M. (1989) J. Physiol. (London) **416**, 349–367
2 Lacy, P. E., Finke, E. H. and Codilla, R. C. (1975) Lab. Invest. **33**, 570–576
3 Somers, G., Blondel, B., Orci, L. and Malaisse, W. J. (1979) Endocrinology **104**, 255–264
4 Augustine, G. J. and Neher, E. (1992) J. Physiol. (London) **450**, 247–271
5 Hisatomi, M., Hidaka, H. and Niki, I. (1996) Endocrinology **137**, 4644–4649
6 Lang, T., Wacker, I., Steyer, J., Kaether, C., Wunderlich, I., Soldati, T., Gerdes, H. H. and Almers, W. (1997) Neuron **18**, 857–863
7 Wacker, I., Kaether, C., Kromer, A., Migala, A., Almers, W. and Gerdes, H. H. (1997) J. Cell Sci. **110**, 1453–1463
8 Pouli, A. E., Kennedy, H. J., Schofield, J. G. and Rutter, G. A. (1998) Biochem. J. **331**, 669–675
9 Heim, R., Cubitt, A. B. and Tsien, R. Y. (1995) Nature (London) **373**, 663–664
10 Wasmeier, C. and Hutton, J. C. (1996) J. Biol. Chem. **271**, 18161–18170
11 Pouli, A. E., Karagenc, N., Arden, S., Bright, N., Schofield, G. S., Hutton, J. C. and Rutter, G. A. (1998) Biochem. J. **330**, 1399–1404
12 Asfari, M., Janjic, D., Meda, P., Li, G., Halban, P. A. and Wollheim, C. B. (1992) Endocrinology **130**, 167–178
13 Sekine, N., Cirulli, V., Regazzi, R., Brown, L. J., Gine, E., Tamarit-Rodriguez, J., Girotti, M., Marie, S., MacDonald, M. J., Wollheim, C. B. and Rutter, G. A. (1994) J. Biol. Chem. **269**, 4895–4902
14 Rutter, G. A., Theler, J.-M., Murta, M., Wollheim, C. B., Pozzan, T. and Rizzuto, R. (1993) J. Biol. Chem. **268**, 22385–22390
15 Greene, L. A. and Tischler, A. S. (1976) Proc. Natl. Acad. Sci. U.S.A. **73**, 2424–2428
16 Rutter, G. A., Burnett, P., Rizzuto, R., Brini, M., Murgia, M., Pozzan, T., Tavare, J. M. and Denton, R. M. (1996) Proc. Natl. Acad. Sci. U.S.A. **93**, 5489–5494
17 Bonner-Weir, S. (1988) Diabetes **37**, 616–621
18 Smith, C. B. and Betz, W. J. (1996) Nature (London) **380**, 531–534
19 Hirokawa, N. (1998) Science **279**, 519–526
20 Kreis, T. E., Matteoni, R., Hollinshead, M. and Tooze, J. (1989) Eur. J. Cell Biol. **49**, 128–139
21 Hurtley, S. M. (1993) J. Cell Sci. **106**, 649–655
22 Rorsman, P. (1997) Diabetologia **40**, 487–495